Solid-State H-2 NMR and MD Simulations of Positional Isomers of a Monounsaturated Phospholipid Membrane: Structural Implications of Double Bond Location

ARTICLE *in* THE JOURNAL OF PHYSICAL CHEMISTRY B · SEPTEMBER 2010

Impact Factor: 3.3 · DOI: 10.1021/jp105068g · Source: PubMed

Solid-State ^{2}H NMR and MD Simulations of Positional Isomers of a Monounsaturated Phospholipid Membrane: Structural Implications of Double Bond Location

Stephen R. Wassall,*,† M. Alan McCabe,† Cynthia D. Wassall,† Richard O. Adlof,‡ and Scott E. Feller§

Department of Physics, Indiana University−Purdue University Indianapolis, Indianapolis, Indiana 46202-3273; US Department of Agriculture, National Center for Agricultural Utilization Research, Peoria, Illinois 61604; and Department of Chemistry, Wabash College, Crawfordsville, Indiana 47933

Received: June 2, 2010; Revised Manuscript Received: July 23, 2010

The impact that the position of double bonds has upon the properties of membranes is investigated using solid-state ^{2}H NMR and MD simulations to compare positional isomers of 1-palmitoyl-2-octadecenoylphosphatidylcholine (16:0-18:1PC) bilayers that are otherwise identical apart from the location of a single *cis* double bond at the Δ^6, Δ^9, Δ^{12}, or Δ^{15} position in the 18:1 *sn*-2 chain. Moment analysis of ^{2}H NMR spectra recorded for isomers perdeuterated in the 16:0 *sn*-1 chain reveals that average order parameters $\bar{S}_{CD}$ change by more than 35% and that the temperature for chain melting T_m varies by 40 °C. At equal temperature, the $\bar{S}_{CD}$ values exhibit a minimum, as do T_m values, when the double bond is in the middle of the 18:1 *sn*-2 chain and increase as it is shifted toward each end. Order parameter profiles generated from depaked ("dePaked") spectra for the 16:0 *sn*-1 chain all possess the same shape with a characteristic "plateau" region of slowly decreasing order in the upper portion before progressively decreasing more in the lower portion. The NMR results are interpreted on the basis of MD simulation results obtained on each of the four systems. The simulations support the idea that the order parameter changes reflect differences in molecular surface areas, and furthermore that the molecular areas are a function of the strength of the acyl chain attractions.

1. Introduction

There is currently tremendous interest in unsaturated phospholipid membranes. The motivation for characterizing such systems at the molecular level is to determine why certain unsaturated fatty acids possess nutritional benefits and/or are essential for biochemical function in specific membranes. A reduced risk for developing coronary heart disease is correlated with the decrease in plasma levels of low-density lipoprotein cholesterol that dietary monounsaturated and polyunsaturated fatty acids (PUFA) tend to produce, for instance, whereas saturated and *trans* (*cis* unsaturation is assumed unless otherwise designated) unsaturated fatty acids tend to have the opposite adverse effect.[1] Docosahexaenoic (22:6) acid, the most unsaturated fatty acid found in nature with 22 carbons and 6 double bonds, has been the subject of particular attention. Claims exist that dietary consumption of this ω-3 PUFA alleviates a vast array of health problems.[2] Its presence in specialized membranes such as neural membranes is essential for protein function that is compromised by replacement with a fatty acid that differs by as little as one fewer double bond.[3]

The conventional approach to studying the impact of unsaturation has been to investigate how varying the number of double bonds affects the properties of model membranes. Differential scanning calorimetry (DSC) showed that the first double bond introduced into the *sn*-2 chain of phosphatidylcholines (PC) with a saturated *sn*-1 chain reduces the temperature of the chain melting transition T_m by on the order of 60 °C.[4,5] A further reduction of approximately 15 °C accompanies addition of the second double bond, and there is then little change in T_m with more double bonds. This same dependence upon number of double bonds in the *sn*-2 chain was corroborated by values for T_m ascertained in moment analysis of ^{2}H NMR spectra from PC with a perdeuterated [$^2H_{35}$]stearoyl (18:0) *sn*-1 chain.[6] Somewhat analogously, the area/molecule measured from pressure−area curves for monolayers of PC with a saturated *sn*-1 chain increases substantially with the addition of each of the first three bonds to the *sn*-2 chain but then changes negligibly when more double bonds are added.[7,8] Order within [$^2H_{35}$]18:0-*X*PC membranes where *X* is an oleic (18:1), linoleic (18:2), linolenic (18:3), arachidonic (20:4), eicosapentaenoic (20:5), or 22:6 acid *sn*-2 chain similarly is relatively insensitive to the number of double bonds at high levels of unsaturation as probed by ^{2}H NMR of the perdeuterated *sn*-1 chain in the liquid crystalline phase.[6,9] While introduction of the second and third double bonds lowers order appreciably, subsequent changes are subtle for bilayers containing 3−6 double bonds.

A structural issue that has been largely ignored is the location of double bonds. Our previous ^{2}H NMR study of 1-[$^2H_{31}$]palmitoyl-2-α-linolenoylphosphatidylcholine ([$^2H_{31}$]16:0-α18:3PC) and 1-[$^2H_{31}$]palmitoyl-2-γ-linolenoylphosphatidylcholine ([$^2H_{31}$]16:0-γ18:3PC) bilayers contrasted isomeric phospholipids that were identical except for having double bonds at respective positions 9, 12, and 15 or 6, 9, and 12.[10] The results unequivocally demonstrated major differences in phase behavior and membrane ordering. [$^2H_{31}$]16:0-α18:3PC exhibited a gel to liquid crystalline transition with temperatures of −9 °C on heating and −20 °C on cooling, while in [$^2H_{31}$]16:0-γ18:3PC the transition at −27 °C was free of observable hysteresis. Average order parameters $\bar{S}_{CD}$ in the liquid crystalline state were 10% smaller in [$^2H_{31}$]16:0-α18:3PC than [$^2H_{31}$]16:0-γ18:3PC at the same

* To whom correspondence should be addressed. Tel: 317 274-6908. Fax: 317 274-2393. E-mail: swassall@iupui.edu.
† Indiana University−Purdue University Indianapolis.
‡ National Center for Agricultural Utilization Research (retired).
§ Wabash College.

10.1021/jp105068g
Published on Web 08/13/2010

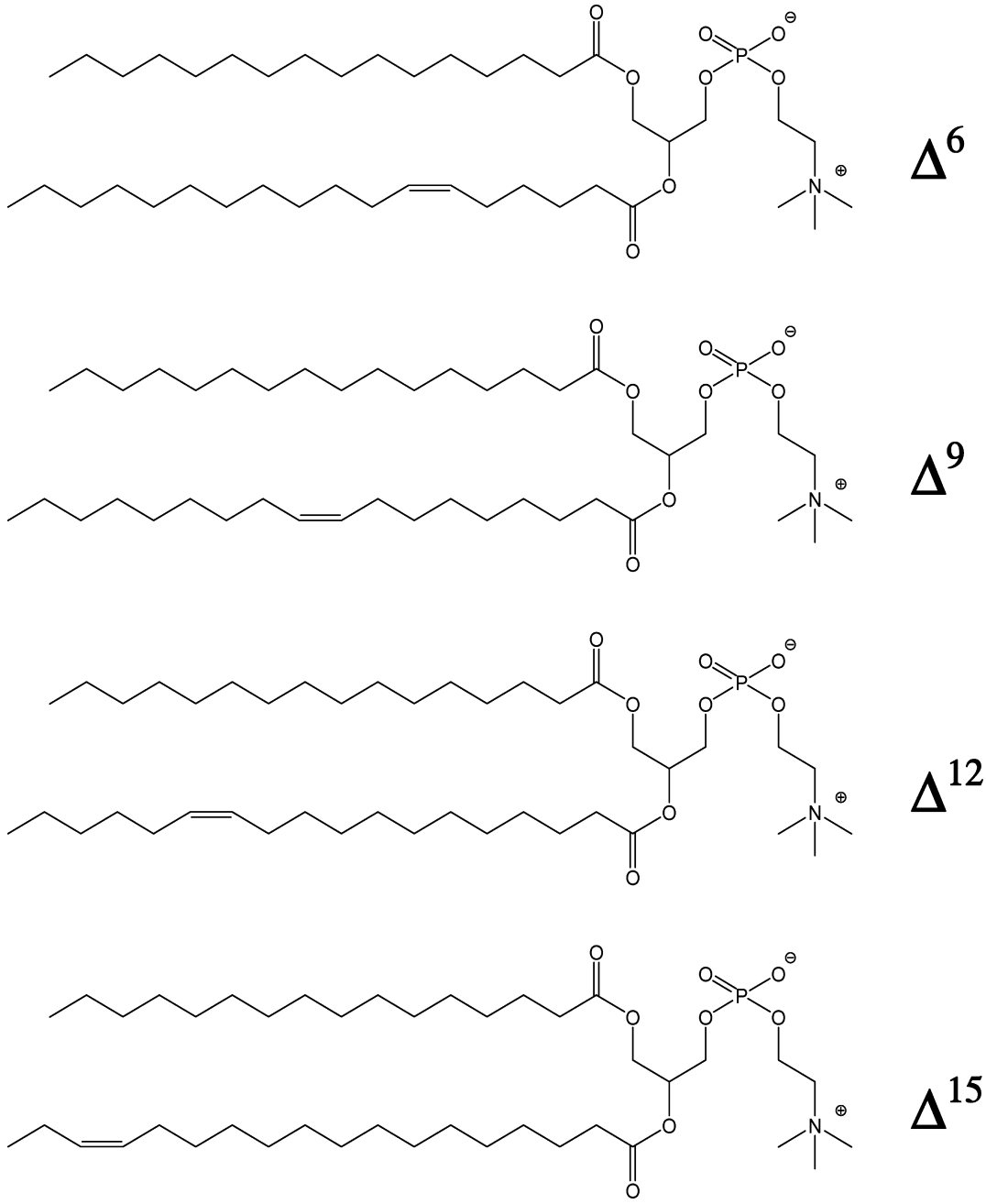

Figure 1. Molecular structure of the Δ^6, Δ^9, Δ^{12}, and Δ^{15} positional isomers of 16:0-18:1PC.

temperature. We also saw differences in fusion, permeability and cholesterol-induced condensation between isomers of closely related 1-stearoyl-2-α-linolenoylphosphatidylcholine (18:0-α18:3PC) vs 1-stearoyl-2-γ-linolenoylphosphatidylcholine (18:0-γ18:3PC). The former phospholpid displayed higher permeability to erythritol in osmotic swelling experiments on multilamellar liposomes and a faster rate of fusion as monitored by fluorescence resonance energy transfer between sonicated unilamellar vesicles.[11] Cholesterol was observed to condense monolayers and bilayers of 18:0-α18:3PC but not 18:0-γ18:3PC.[12] The results of these studies clearly establish that the location of double bonds, as well as the number, contributes to membrane properties in a complex manner.

In this investigation we employ the techniques of solid-state ^{2}H NMR and molecular dynamics (MD) computer simulation to compare 1-[$^2H_{31}$]palmitoyl-2-octadecenoylphosphatidylcholine ([$^2H_{31}$]16:0-18:1PC) bilayers with the double bond situated at the 6, 9, 12, or 15 position of the 18:1 *sn*-2 chain. As illustrated in Figure 1, the well-defined, isomeric nature of the monounsaturated phospholipid ensures that the position of a single double bond is the only structural variable. The physiologically prevalent Δ^9 isomer serves as a benchmark for comparison. By ^{2}H NMR of the [$^2H_{31}$]16:0 *sn*-1 chain, phase behavior and order within the membrane are noninvasively probed. Earlier DSC work on phospholipid membranes with saturated *sn*-1 and monounsaturated *sn*-2 chains or identical monounsaturated *sn*-1 and -2 chains revealed that the temperature T_m of the chain melting transition is critically dependent upon position of the double bond.[13−15] The temperature is a minimum when the double bond is near the center of the chain and increases progressively as the bond is located toward either end. Our results here on positional isomers of [$^2H_{31}$]16:0-18:1PC elaborate upon the phase behavior seen by calorimetry and identify how molecular organization within the membrane in

the liquid crystalline state is influenced by the location of the double bond in the 18:1 *sn*-2 chain. Interpretation of the NMR data based on molecular dynamics simulations performed on each of the four systems supports the idea that changes in order parameter reflect differences in molecular surface areas, and furthermore that the molecular areas are a function of the strength of the acyl chain attractions.

2. Experimental Methods

2.1. Materials. Positional isomers of 1-[$^2H_{31}$]palmitoyl-2-*cis*-octadeca-n_u-enoylphosphatidylcholine ([$^2H_{31}$]16:0-18:1Δ^nPC) where $n = 6$, 9, 11, 12, or 15 specifies the location of the double bond were obtained by custom synthesis from Avanti Polar Lipids (Alabaster, AL). We supplied 12-*cis* and 15-*cis*-octadecenoic acids. They were prepared by the reduction of methyl linolenate with hydrazine.[16] The *cis*-monoenoic methyl ester fraction (a mixture of 36.6% 9-*cis*-18:1, 36.6% 12-*cis*-18:1 and 26.8% 15-*cis*-18:1) was isolated by counter current distribution (CCD) using a silver nitrate solvent system[17] and fractionated by elution through a glass 3 × 30 cm Michael Miller column packed with 200/270 mesh XN1010 resin (Ag^+ form), methanol (4 mL/min) as eluting solvent and UV detection at 206 nm.[18] Repeated fractionation (a total of seven times) yielded the 15-cis isomer in 99.6% purity. The more difficult separation of the 9-*cis*-18:1/12-*cis*-18:1 isomer pair was accomplished following repeated fractionation by CCD and silver resin chromatography to finally yield the 12-*cis* isomer in 99.1% purity. Sigma (St. Louis, MO) or Isotec (Miamisburg, OH) was the source of deuterium depleted water.

2.2. Sample Preparation. The NMR samples consisted of aqueous multilamellar dispersions of 50% by weight phospholipid in 20 mM Tris buffer (pH 7.5). Stock solutions of 80−100 mg of phospholipid in chloroform were initially dried under nitrogen, followed by vacuum pumping for 10−12 h to remove residual solvent. The appropriate volume of buffer was added to the dried phospholipids and multilamellar dispersions were prepared in the presence of excess (2 mL) deuterium depleted water by vortex mixing at a temperature above the gel to liquid crystalline phase transition for several minutes. The pH was adjusted and three lyophilizations were then performed to reduce the residual ^2H NMR signal from natural abundance ^2HHO. To avoid oxidation of the monounsaturated lipids, the various manipulations were carried out under a stream of nitrogen, the water was degassed, and exposure to direct light was minimized. The resultant samples were transferred to 5 mm NMR tubes and stored at −20 °C. They were always equilibrated at room temperature for at least 1 h prior to experimentation.

2.3. ^2H NMR. Solid-state ^2H NMR spectra for [$^2H_{31}$]16:0-18:1Δ^nPC were acquired on a home-built spectrometer operating at a resonance frequency of 27.6 MHz.[19] A probe with a 5 mm transverse mounted coil (Cryomagnet Systems, Indianapolis, IN) was utilized. Temperature was regulated (±0.5 °C) with a Love Controls (1600 series) temperature controller (Michigan City, IN). The data were collected in quadrature with a phase-alternated quadrupolar echo sequence $(90°_x-\tau_2-90°_y-\text{acquire}-\text{delay})_n$.[20] Typical spectral parameters were 90° pulse width ≈2.5 μs; separation between pulses $\tau = 50$ μs; delay between pulse sequences = 1.0 and 1.5 s in the gel and liquid crystalline phases, respectively; sweep width = ±250 and ±100 kHz in the respective phases; line broadening = 125 and 50 Hz in the respective phases; data set = 2K; and number of transients = 1024.

The first moment M_1 was calculated from ^2H NMR spectra with

$$M_1 = \frac{\int_{-\infty}^{\infty} |\omega| f(\omega)\, d\omega}{\int_{-\infty}^{\infty} f(\omega)\, d\omega} \tag{1}$$

where ω is the frequency with respect to the central Larmor frequency ω_0 and $f(\omega)$ is the line shape.[21] In practice, the integral is a summation over the digitized data and the reproducibility of the values obtained is usually ±1%. The expression

$$M_1 = \frac{\pi}{\sqrt{3}}\left(\frac{e^2qQ}{h}\right)|\bar{S}_{CD}| \tag{2}$$

relates M_1 to the average order parameter $\bar{S}_{CD}$ of the perdeuterated [$^2H_{31}$]16:0 *sn*-1 chain in the liquid crystalline state via the static quadrupolar coupling constant (e^2qQ/h) = 167 kHz. The order parameter S_{CD} is defined according to

$$S_{CD} = {}^1/_2\langle 3\cos^2\beta - 1\rangle \tag{3}$$

where β is the time-dependent angle between a C−^2H bond and the bilayer normal, and the angular brackets denote a time average.[22] Values in the range $0 \le |S_{CD}| \le {}^1/_2$ are taken for a saturated chain, the respective limits representing effective isotropic motion and fast axial rotation in all-*trans* configuration.

Spectra were also FFT depaked ("dePaked") to enhance resolution in the liquid crystalline phase. The depaking algorithm numerically deconvolutes the powder pattern signal to a spectrum representative of a planar membrane of single alignment.[19] The depaked spectra consist of doublets with quadrupolar splittings $\Delta\nu(\theta)$ that equate to order parameters by

$$\Delta\nu(\theta) = \frac{3}{2}\left(\frac{e^2qQ}{h}\right)|S_{CD}|P_2(\cos\theta) \tag{4}$$

where $\theta = 0°$ is the angle the membrane normal makes with the magnetic field and $P_2(\cos\theta)$ is the second-order Legendre polynomial. Smoothed profiles of order along the [$^2H_{31}$]16:0 *sn*-1 chain were then generated assuming monotonic variation toward the disordered center of the bilayer.[23]

2.4. MD Simulations. Simulations were carried out following the procedure established previously for the study of unsaturated PC.[24,25] The program CHARMM[26] was used for system construction, simulation, and analysis, with the CHARMM lipid force field.[27] The starting configuration for the Δ^9 isomer was taken from the end of an earlier simulation,[28] while the other isomers were prepared from this same configuration by removing/adding appropriate hydrogen atoms and applying a harmonic restraint to the C−C=C−C torsion to drive each system into the *cis* isomer at the desired position. Each system consisted of 72 lipid molecules and 1440 water molecules. All simulations were carried out with the identical fixed molecular surface area (65.2 Å^2/molecule) under conditions of constant normal pressure (1 atm) and a constant temperature (40 °C). By carrying out all simulations at equal molecular area, the lateral tension can be computed and used as a measure of the tendency of the system to contract or expand its area. Simulations were carried out for 40 ns with the initial 10 ns discarded as equilibration, using a 2 fs time step. Electrostatic forces were computed with the smooth particle mesh Ewald method,[29] bonds involving hydrogen atoms were constrained by means of the SHAKE algo-

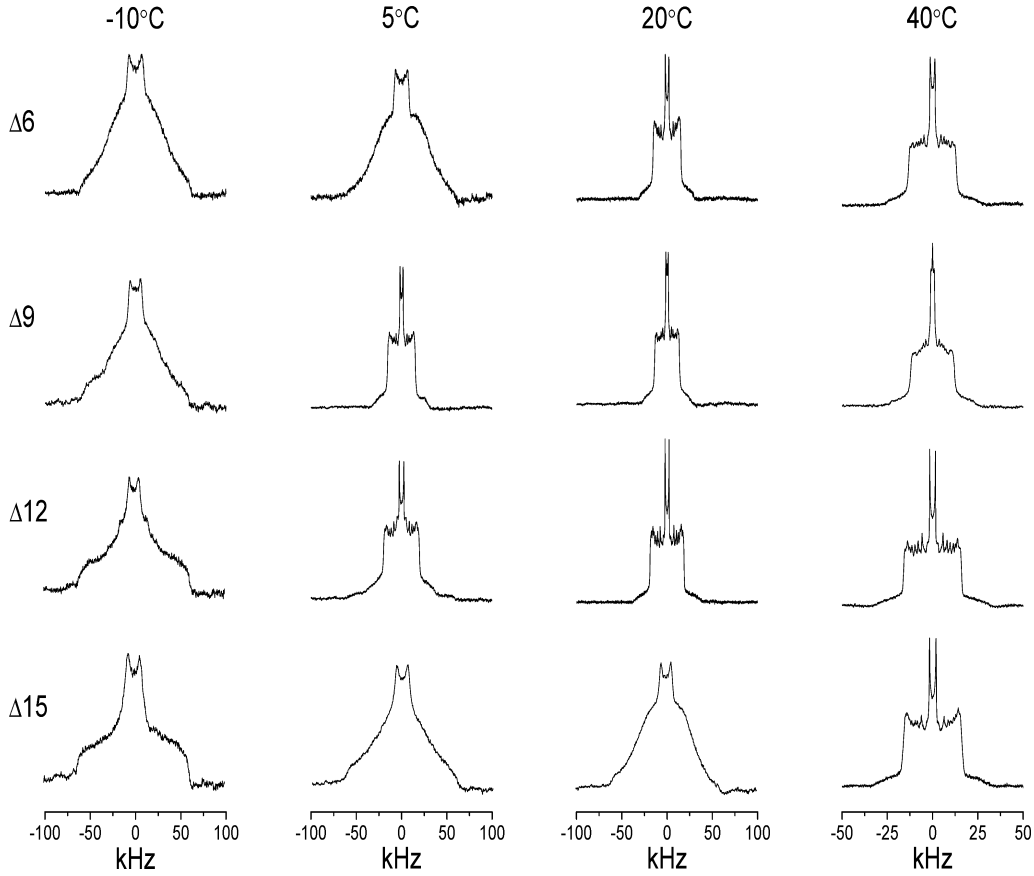

Figure 2. ^2H NMR spectra for 50 wt % aqueous dispersions in 20 mM Tris (pH 7.5) of [$^2H_{31}$]16:0-18:1Δ^{6}PC, [$^2H_{31}$]16:0-18:1Δ^{9}PC, [$^2H_{31}$]16:0-18:1Δ^{12}PC, and [$^2H_{31}$]16:0-18:1Δ^{15}PC.

rithm,[30] and conformations were saved once per picosecond for subsequent analysis.

3. Results

3.1. ^2H NMR. ^2H NMR spectra for aqueous dispersions of [$^2H_{31}$]16:0-18:1Δ^{6}PC, [$^2H_{31}$]16:0-18:1Δ^{9}PC, [$^2H_{31}$]16:0-18:1Δ^{12}PC, and [$^2H_{31}$]16:0-18:1Δ^{15}PC were collected as a function of temperature. Illustrative examples are presented in Figure 2. At the lowest temperature of −10 °C shown, the spectra for all four isomers are broad and relatively featureless with shoulders at ±63 kHz. They are characteristic of the gel phase where the [$^2H_{31}$]16:0 *sn*-1 chains are all-*trans* and reorient slowly.[21] The much narrower spectra at the highest temperature of 40 °C shown indicate that each isomer has undergone a phase transition into the liquid crystalline state where *trans*−*gauche* isomerization about C−C bonds produces fast axial reorientation for the acyl chains.[21] There are well-defined edges at ∼±15 kHz that correspond to the plateau region of almost constant order in the upper portion of the [$^2H_{31}$]16:0 *sn*-1 chain. The individual peaks within the spectrum arise from the less ordered methylenes in the lower part of the chain, and the central pair of peaks is due to the highly mobile terminal methyl group. At the intermediate temperatures displayed, in contrast, the spectra clearly demonstrate that the four isomers do not adopt the same phase. The spectra for [$^2H_{31}$]16:0-18:1Δ^{9}PC and [$^2H_{31}$]16:0-18:1Δ^{12}PC at 5 °C are liquid crystalline in form, whereas the spectra for [$^2H_{31}$]16:0-18:1Δ^{6}PC and [$^2H_{31}$]16:0-18:1Δ^{15}PC remain symptomatic of the gel phase. On raising the temperature further to 20 °C, the spectra establish that [$^2H_{31}$]16:0-18:1Δ^{6}PC as well as [$^2H_{31}$]16:0-18:1Δ^{9}PC and [$^2H_{31}$]16:0-18:1Δ^{12}PC has become liquid crystalline but [$^2H_{31}$]16:0-18:1Δ^{15}PC is still gel.

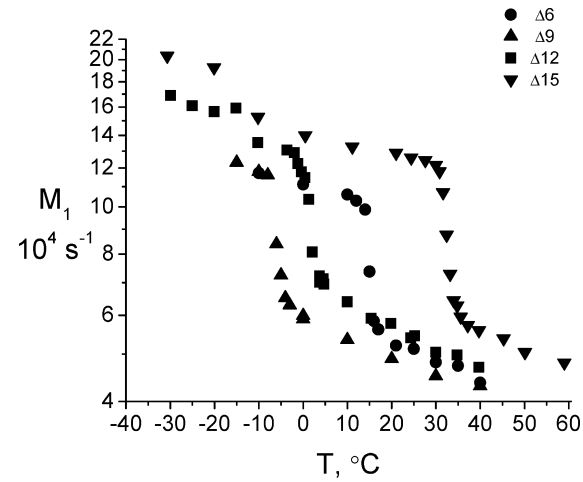

Figure 3. Variation of the first moment M_1 with temperature for 50 wt % aqueous dispersions in 20 mM Tris (pH 7.5) of (●) [$^2H_{31}$]16:0-18:1Δ^{6}PC, (▲) [$^2H_{31}$]16:0-18:1Δ^{9}PC, (■) [$^2H_{31}$]16:0-18:1Δ^{12}PC, and (▼) [$^2H_{31}$]16:0-18:1Δ^{15}PC.

A dependence of the temperature for the chain melting transition upon the location of the double bond is responsible for the differences between spectra recorded in Figure 2 for the positional isomers of [$^2H_{31}$]16:0-18:1PC. First moments M_1 calculated from the spectra with eq 1 for [$^2H_{31}$]16:0-18:1Δ^{6}PC, [$^2H_{31}$]16:0-18:1Δ^{9}PC, [$^2H_{31}$]16:0-18:1Δ^{12}PC, and [$^2H_{31}$]16:0-18:1Δ^{15}PC are plotted against temperature in Figure 3 to elaborate the phase behavior. In each case an abrupt drop in value associated with the transition from gel ($M_1 > 10 \times 10^4$ s^{-1}) to liquid crystalline ($M_1 < 6 \times 10^4$ s^{-1}) phase is apparent. The vast disparity between the temperatures of the transition,

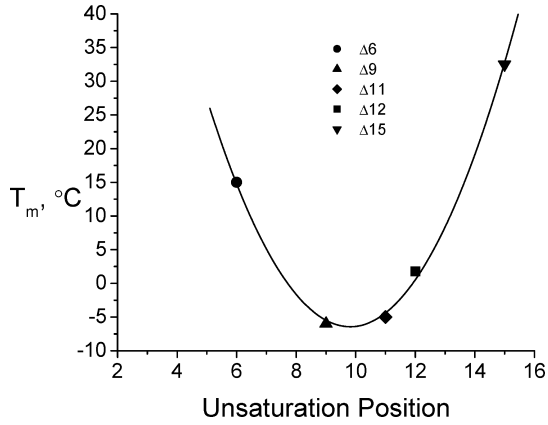

Figure 4. Dependence upon position of unsaturation for the temperature T_m of the chain melting transition for (●) [$^2H_{31}$]16:0-18:1Δ^6PC, (▲) [$^2H_{31}$]16:0-18:1Δ^9PC, (■) [$^2H_{31}$]16:0-18:1Δ^{12}, and (▼) [$^2H_{31}$]16:0-18:1Δ^{15}PC. Included in the plot is a T_m value for (◆) [$^2H_{31}$]16:0-18:1Δ^{11}PC (Thewalt, private communication). A least-squares polynomial fit is drawn through the data.

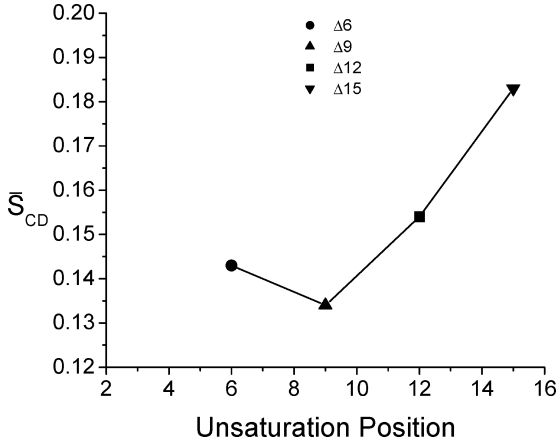

Figure 5. Dependence upon position of unsaturation for the average order parameter $\bar{S}_{CD}$ for (●) [$^2H_{31}$]16:0-18:1Δ^6PC, (▲) [$^2H_{31}$]16:0-18:1Δ^9PC, (■) [$^2H_{31}$]16:0-18:1Δ^{12}PC, and (▼) [$^2H_{31}$]16:0-18:1Δ^{15}PC at 40 °C.

moreover, is evident. The Δ^9 isomer melts at the lowest temperature with a transition that is ~2 °C in width and centered on $T_m = -6$ °C. A move of the double bond in either direction away from the 9 position in the middle of the 18:1 *sn*-2 chain increases T_m. When the unsaturation is closer to the glycerol backbone in [$^2H_{31}$]16:0-18:1Δ^6PC, $T_m = 15$ °C. For [$^2H_{31}$]16:0-18:1Δ^{12}PC and [$^2H_{31}$]16:0-18:1Δ^{15}PC the transition occurs, respectively, at 2 and 32 °C with the double bond progressively closer to the terminal methyl. The U-like trend, which is consistent with DSC work,[13−15] is summarized graphically in Figure 4.

Average order parameters $\bar{S}_{CD}$ for the monounsaturated phospholipids were derived from first moments M_1 in the liquid crystalline state according to eq 2. Figure 5 reports how $\bar{S}_{CD}$ is affected by the position of the double bond at 40 °C. The variation is appreciable, qualitatively paralleling that seen for the temperature of the chain melting transition T_m in Figure 4. Order within the [$^2H_{31}$]16:0 *sn*-1 chain is a minimum, corresponding to the greatest disruption to molecular organization, when the double bond is at the center of the neighboring 18:1 *sn*-2 chain between carbons 9 and 10. The disordering due to the double bond is reduced when it is relocated to the 6, 12, or 15 position. The differential relative to [$^2H_{31}$]16:0-18:1Δ^9PC is particularly marked for [$^2H_{31}$]16:0-18:1Δ^{15}PC. The value of $\bar{S}_{CD}$ is >35% bigger for the Δ^{15} isomer.

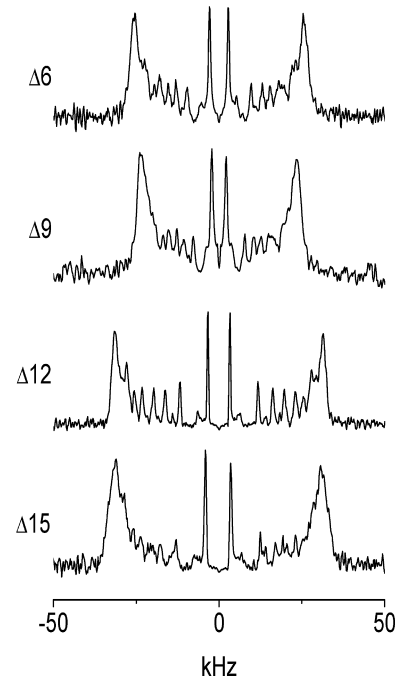

Figure 6. FFT depaked ^2H NMR spectra for 50 wt % aqueous dispersions in 20 mM Tris (pH 7.5) of [$^2H_{31}$]16:0-18:1Δ^6PC, [$^2H_{31}$]16:0-18:1Δ^9PC, [$^2H_{31}$]16:0-18:1Δ^{12}PC, and [$^2H_{31}$]16:0-18:1Δ^{15}PC at 40 °C.

FFT depaked spectra[19] for [$^2H_{31}$]16:0-18:1Δ^6PC, [$^2H_{31}$]16:0-18:1Δ^9PC, [$^2H_{31}$]16:0-18:1Δ^{12}PC, and [$^2H_{31}$]16:0-18:1Δ^{15}PC at 40 °C are displayed in Figure 6. They consist of an outermost composite doublet and five to six well-resolved doublets. Ordered methylenes in the upper portion of the chain produce the outermost doublet while the individual doublets are, with decreasing splitting, sequentially due to the disordered methylenes and terminal methyl in the lower portion of the chain. The enhancement in resolution accomplished facilitates more sophisticated analysis in terms of a smoothed profile of order along the [$^2H_{31}$]16:0 *sn*-1 chain.[23] The procedure equates the splitting of doublets to order parameter S_{CD} via eq 4, assigning equal integrated intensity to each methylene in the perdeuterated chain and assuming order decreases monotonically toward the terminal methyl.

The order parameters calculated as a function of acyl chain position from the FFT depaked spectra for [$^2H_{31}$]16:0-18:1Δ^6PC, [$^2H_{31}$]16:0-18:1Δ^9PC, [$^2H_{31}$]16:0-18:1Δ^{12}PC, and [$^2H_{31}$]16:0-18:1Δ^{15}PC at 40 °C are drawn in Figure 7. All four profiles are of the same shape that is a signature for the saturated *sn*-1 chain in homoacid disaturated PC or heteroacid saturated−unsaturated PC membranes in the liquid crystalline phase.[6,22] They have a plateau region of approximately constant order in the upper portion of the chain (C2−9) followed by progressively decreasing order in the lower portion (C10−16). Thus, Figure 7 establishes that a shift in position of the double bond in the 18:1 *sn*-2 chain of the monounsaturated phospholipid is accompanied by changes in order throughout the [$^2H_{31}$]16:0 *sn*-1 chain that maintain the characteristic overall form of profile. In accordance with the measurements of $\bar{S}_{CD}$ (Figure 5), order is depressed most for the Δ^9 isomer and becomes less so for the Δ^6, Δ^{12}, and Δ^{15} isomers.

3.2. MD Simulations. Figure 8 gives the order parameters for the *sn*-1 and -2 chains computed from the MD simulations for 16:0-18:1Δ^6PC, 16:0-18:1Δ^9PC, 16:0-18:1Δ^{12}PC, and 16:0-18:1Δ^{15}PC at 40 °C. The data for the *sn*-1 chain (Figure 8a)

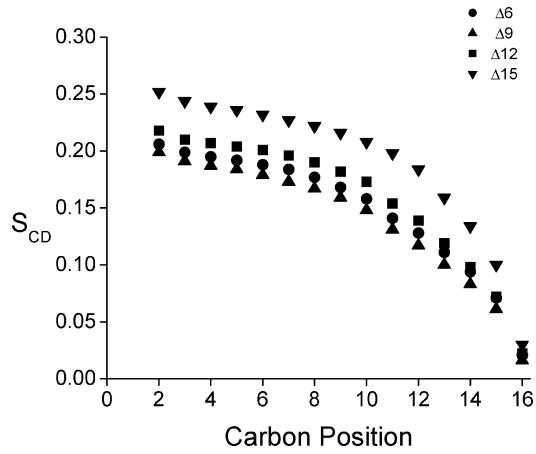

Figure 7. Smoothed profile of order parameter S_{CD} vs position along the *sn*-1 chain for (●) [$^2H_{31}$]16:0-18:1Δ^6PC, (▲) [$^2H_{31}$]16:0-18:1Δ^9PC, (■) [$^2H_{31}$]16:0-18:1Δ^{12}PC, and (▼) [$^2H_{31}$]16:0-18:1Δ^{15}PC at 40 °C derived from FFT depaked spectra.

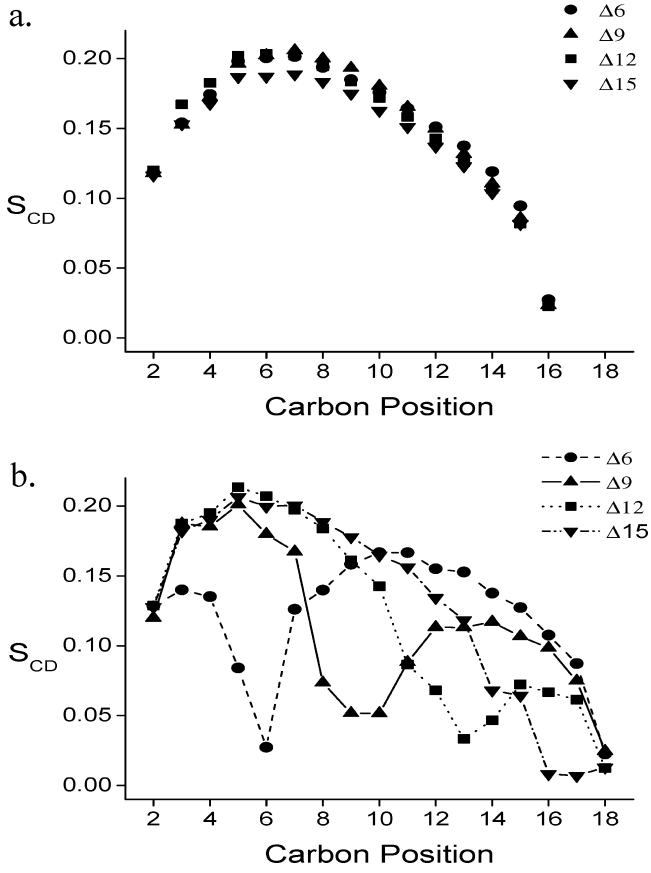

Figure 8. Profile of order parameter S_{CD} vs position along the *sn*-1 (a) and -2 (b) chains for (●) 16:0-18:1Δ^6PC, (▲) 16:0-18:1Δ^9PC, (■) 16:0-18:1Δ^{12}PC, and (▼) 16:0-18:1Δ^{15}PC at 40 °C derived from MD simulated data.

are characteristic of a saturated chain, in agreement with experiment reproducing a profile comprised of a plateau region with $|S_{CD}| \sim 0.2$ followed by a gradual decrease in order parameter as the terminal methyl group is approached.[22] The similarity in shape for each isomer, as is also displayed by our experimental NMR measurements (Figure 7), implies that local perturbation of the environment of the CH_2 segments is small; i.e., the presence of the double bond does not alter the conformations of the *sn*-1 chain segments in its immediate vicinity. The profiles differ from those observed experimentally in that the simulated *sn*-1 chain profiles do not shift in overall magnitude of the plateau region in response to changes in position of the double bond of the *sn*-2 chain. This result, however, is to be expected given our choice of a constant, and identical, surface area for all simulations. The simulations thus support interpretation of shifts in experimentally observed order parameters as arising from changes in molecular surface area. The slight lowering of the profile for the Δ^{15} isomer suggests that the unsaturated *sn*-2 chain may have a somewhat lower chain surface area requirement, allowing the saturated chain area to expand slightly in this case.

The order parameters computed from the MD simulations for the *sn*-2 chain exhibit profiles for the four positional isomers that are quite distinct from one another (Figure 8b) and from the saturated *sn*-1 chain (Figure 8a). There is a dip in order parameter in the vicinity of the double bond for each isomer. Far from the site of unsaturation, the profiles begin to resemble the profile of the saturated chain; e.g., there is a plateau region ($|S_{CD}| \sim 0.2$) in the upper portion of chains with a double bond at positions 12 and 15 in the lower half. A similar trend is apparent in MD simulated data reported for positional isomers of 1,2-dioctadecenoylphosphatidylcholine (18:1-18:1PC) with identical *sn*-1 and -2 chains.[31] The drop in order parameter seen in our simulated profile near the site of unsaturation in 16:0-18:1Δ^9PC qualitatively resembles that reported experimentally in ^2H NMR work.[32] Extremely high disorder within the unsaturated chain is not the reason. Taking into account geometrical factors, analysis of ^2H NMR splittings measured for 9 and 10 positions established that an average orientation close to the bilayer normal for the *cis* double bond is responsible. Quantitative comparison of the small S_{CD} value at the double bond position obtained by simulation and experiment for the Δ9 isomer and by simulation for the different isomers is challenging because the uncertainty in the order parameter calculation, as measured by the standard deviation among the 72 chains simulated, is relatively high. The C6 and C9 positions of the Δ6 and Δ9 isomers where $S_{CD} = 0.03 \pm 0.05$ and 0.05 ± 0.06, respectively, exemplify the problem.

4. Discussion

Solid-state ^2H NMR spectra were recorded for [$^2H_{31}$]16:0-18:1Δ^6PC, [$^2H_{31}$]16:0-18:1Δ^9PC, [$^2H_{31}$]16:0-18:1Δ^{12}PC, and [$^2H_{31}$]16:0-18:1Δ^{15}PC. These four positional isomers differ only in where the double bond is placed. Analysis of the spectra reveals how the temperature of the chain melting transition and, for the first time, order within the bilayer is affected by the location of the double bond in the monounsaturated 18:1 *sn*-2 chain. Insight into the mechanism by which order is changed when the double bond is moved was then gleaned from MD simulations that were performed on the same positional isomers.

4.1. Chain Melting Behavior. The temperature of the gel to liquid crystalline phase transition for [$^2H_{31}$]16:0-18:1Δ^6PC, [$^2H_{31}$]16:0-18:1Δ^9PC, [$^2H_{31}$]16:0-18:1Δ^{12}PC, and [$^2H_{31}$]16:0-18:1Δ^{15}PC is markedly sensitive to the location of the double bond in the 18:1 *sn*-2 chain. This sensitivity is evident from the line narrowing that accompanies the melting of the [$^2H_{31}$]16:0 *sn*-1 chain at the transition in the spectra shown in Figure 2. A broad featureless spectrum that is characteristic of the gel phase was observed with each isomer at −10 °C, the lowest temperature. The spectra for [$^2H_{31}$]16:0-18:1Δ^9PC and [$^2H_{31}$]16:0-18:1Δ^{12}PC narrow and become symptomatic of the liquid crystalline phase upon raising the temperature to 5 °C, while the spectra for [$^2H_{31}$]16:0-18:1Δ^6PC and [$^2H_{31}$]16:0-18:1Δ^{15}PC remain gel-like. At 20 °C, another 15 °C higher in temperature, the spectrum

for [$^2H_{31}$]16:0-18:1Δ^6PC, as well [$^2H_{31}$]16:0-18:1Δ^9PC and [$^2H_{31}$]16:0-18:1Δ^{12}PC, is liquid-crystalline-like and only the spectrum [$^2H_{31}$]16:0-18:1Δ^{15}PC is still indicative of the gel state. The spectra at 40 °C, the highest temperature, then indicate that all 4 isomers, including [$^2H_{31}$]16:0-18:1Δ^{15}PC, are melted.

Precise measurement of the temperature of chain melting T_m for [$^2H_{31}$]16:0-18:1Δ^6PC, [$^2H_{31}$]16:0-18:1Δ^9PC, [$^2H_{31}$]16:0-18:1Δ^{12}PC,and [$^2H_{31}$]16:0-18:1Δ^{15}PC is obtained from the plot of first moment M_1 against temperature presented in Figure 3. A sharp drop in moment signifying the transition from gel to liquid crystalline state, with midpoint designated T_m, is observed at distinctly different temperature for each isomer. As was qualitatively inferred from inspection of the spectra (Figure 2), [$^2H_{31}$]16:0-18:1Δ^9PC (−6 °C) melts at the lowest temperature while [$^2H_{31}$]16:0-18:1Δ^6PC (15 °C), [$^2H_{31}$]16:0-18:1Δ^{12}PC (2 °C), and [$^2H_{31}$]16:0-18:1Δ^{15}PC (32 °C) melt at higher temperature. The transition temperatures measured here for [$^2H_{31}$]16:0-18:1Δ^9PC and [$^2H_{31}$]16:0-18:1Δ^6PC coincide, allowing for the depression in temperature by a few degrees associated with perdeuteration,[33] with those measured by DSC.[15] To the best of our knowledge, a transition temperature has not previously been reported for 16:0-18:1Δ^{12}PC or 16:0-18:1Δ^{15}PC. An interesting point of reference is provided by the transition temperature that was reported for 16:0-18:0PC (1-palmitoyl-2-stearoylphosphatidycholine),[14] the saturated counterpart of 16:0-18:1PC. Its value (T_m = 48.8 °C) indicates that the double bond has a rather limited influence on the transition temperature in the case of the Δ^{15} isomer for which we measured the highest T_m.

In Figure 4, the values of T_m for the different isomers of [$^2H_{31}$]16:0-18:1PC are plotted against the position of the double bond in the 18:1 *sn*-2 chain. They are fitted to a polynomial curve that has a minimum when the double bond is near the middle of the chain and increases when the double bond is moved toward either the upper or lower end of the chain. Similar behavior was seen by Wang and co-workers[34,35] in DSC work on other monoenoic phospholipids and, with the aid of energy-minimized structures, was explained by a simple model.[14] According to the model, the monounsaturated *sn*-2 chain adopts a crankshaft-like motif in the gel state. A $g^{\pm}s^{\pm}\Delta s^{\pm}$ or $s^{\pm}\Delta s^{\pm}g^{\pm}$ sequence of rotational states ($s^{\pm}$ and $g^{\pm}$ specify, correspondingly, *skew*(±) and *gauche*(±) conformation) around the rigid *cis* double (Δ) bond creates a kink that separates a long linear segment in which all of the single C−C bonds are in *trans* conformation and a short disordered segment containing both *trans* and *gauche* rotamers. It is intra- and intermolecular van der Waal's attractive interactions between the longer linear segment and neighboring all-*trans* saturated *sn*-1 chains that stabilize the gel state. These interactions are least when the double bond is close to the middle of the chain because the long linear segment then has minimal length. When the double bond moves away from the center toward either the carbonyl or terminal methyl end of the *sn*-2 chain, the long linear segment becomes greater in length and there is an increase in van der Waal's interactions and a resultant elevation of T_m.

4.2. Acyl Chain Order. That the introduction of a single unsaturation increases membrane disorder in the physiologically relevant liquid crystalline state is well documented.[32] A reduced energy barrier to rotation about the C−C single bonds either side of the C=C double bond, which more than compensates for the rigidity of the double bond, confers greater flexibility upon the monounsaturated chain.[36] Line-shape analysis of the spectra obtained here with [$^2H_{31}$]16:0-18:1Δ^6PC, [$^2H_{31}$]16:0-18:1Δ^9PC, [$^2H_{31}$]16:0-18:1Δ^{12}PC, and [$^2H_{31}$]16:0-18:1Δ^{15}PC at 40 °C (Figure 2) reveals that the amount of disordering exerted upon the saturated *sn*-1 chain is determined by the location of the double bond in the monounsaturated *sn*-2 chain. Average order parameters $\bar{S}_{CD}$ for the [$^2H_{31}$]16:0 *sn*-1 chain, calculated from the first moments for the spectra, exhibit a minimum when the double bond is at the 9 position ($\bar{S}_{CD}$ = 0.134) and rise as the double bond is moved either up ($\bar{S}_{CD}$ = 0.143 at the 6 position) or down ($\bar{S}_{CD}$ = 0.154 and 0.183 at positions 12 and 15, respectively) the 18:1 *sn*-2 chain. This variation is plotted in Figure 5. The order profiles presented in Figure 7 that were constructed from depaked spectra (Figure 6) demonstrate the change in order is global throughout the entire [$^2H_{31}$]16:0 *sn*-1 chain. Despite appreciable difference in average order, the characteristic plateau region of slowly decreasing order in the upper portion (C2−10) followed by a more rapid drop-off in the lower portion (C11−16) is retained with each isomer.

The dependence upon the position of the double bond manifest by $\bar{S}_{CD}$ (Figure 5), in particular the minimal value in the middle of the chain, is similar to that seen for T_m (Figure 4). Like the model proposed by Huang and co-workers[14] to explain the variation of T_m, we also invoke an interpretation for how $\bar{S}_{CD}$ varies in terms of the separation of the 18:1 *sn*-2 chain into long and short saturated sections due to the double bond. When the double bond is near the middle of the chain, the length of the longer section is least and the order of the chain is minimized. Moving the double bond away from the middle of the chain, up toward the carbonyl or down toward the terminal methyl, increases the length of the longer section and the chain becomes more ordered. Lending support to this proposal, order parameters calculated from MD simulated data for the *sn*-1 and -2 chains in positional isomers of 18:1-18:1PC decrease as the double bond is shifted from the membrane surface to the middle of the chain and then increase as the double bond is moved to the terminal methyl end.[31] The MD simulations performed on positional isomers of 16:0-18:1PC under conditions of identical molecular area in this work are now examined to provide further insight into the structural implications of double bond location.

4.3. Lateral Tension. By fixing the molecular surface area for each isomer of 16:0-18:1PC at the value estimated for the Δ^9 isomer, we can investigate whether the increased order observed experimentally with the other positional isomers results from a reduction in molecular area or from changes in conformation of the *sn*-1 chain. If the free energy of the bilayer is lowered by contracting the surface area, we expect a lateral tension to develop in the Δ^6, Δ^{12}, and Δ^{15} isomers above that observed for Δ^9. Figure 9 shows that this is indeed the case with an increased tension observed upon moving the double bond nearer to either end of the acyl chain. The similarity in shape of the curves given in Figure 5 ($\bar{S}_{CD}$ vs unsaturation location) and Figure 9 (lateral tension vs unsaturation location) can be understood on the basis of both quantities being a function of the molecular surface area. Defining A^* as the surface area of the Δ^9 isomer, i.e., the area to which each simulation was constrained, and A_i as the area of the *i*th isomer at its free energy minimum, then the expected tension is related to the area compressibility modulus K_A by

$$\tau_i = -K_A\left(\frac{A_i - A^*}{A^*}\right) \tag{5}$$

The area can also be related to ^2H NMR order parameter S_{CD} by one of a number of similar expressions[37] that relate change in area to change in the projected length, *l*, of the chain along

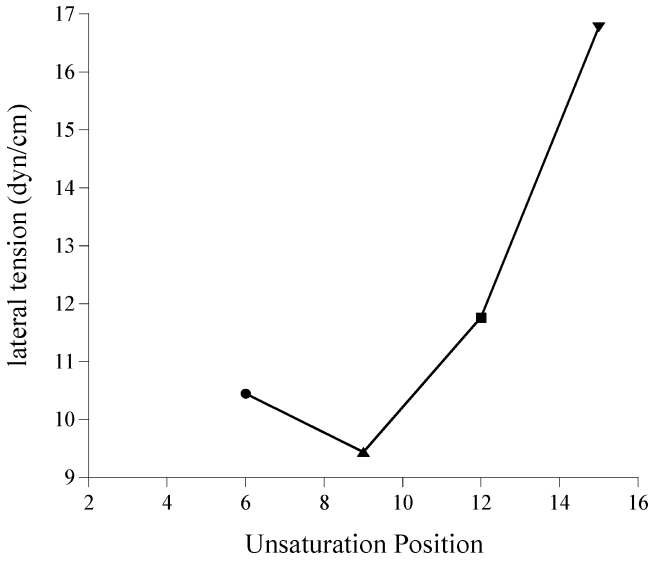

Figure 9. Lateral tension vs position of unsaturation for (●) 16:0-18:1Δ^{6}PC, (▲) 16:0-18:1Δ^{9}PC, (■) 16:0-18:1Δ^{12}PC, and (▼) 16:0-18:1Δ^{15}PC at 40 °C.

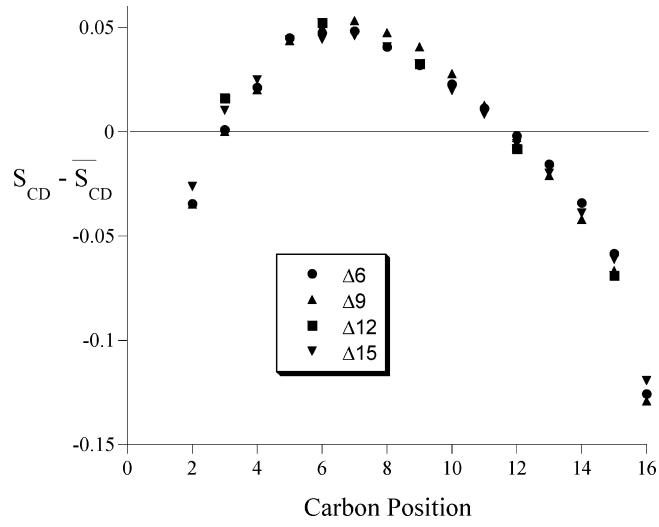

Figure 10. Order parameter profile $S_{CD} - \bar{S}_{CD}$ vs position along the *sn*-1 chain for (●) 16:0-18:1Δ^{6}PC, (▲) 16:0-18:1Δ^{9}PC, (■) 16:0-18:1Δ^{12}PC, and (▼) 16:0-18:1Δ^{15}PC at 40 °C derived from MD simulated data.

the bilayer normal assuming constant chain volume (i.e., $l_1A_1 = l_2A_2$). Plugging $A_i = (l^*/l_i)A^*$ into eq 5 gives

$$\tau_i = -K_A\left(\frac{\frac{l^*}{l_i}A^* - A^*}{A^*}\right) = -K_A\left(\frac{l^*}{l_i} - 1\right) \qquad (6)$$

Equating the projected length to the average order parameter via $l \propto ({}^1/_2 + |\bar{S}_{CD}|)$,[36] then gives

$$\tau_i = \frac{K_A(|\bar{S}^i_{CD}| - |\bar{S}^*_{CD}|)}{{}^1/_2 + |\bar{S}^i_{CD}|} \qquad (7)$$

Recognizing that the denominator of eq 7 is roughly constant for the systems under investigation, it is thus expected that changes in lateral tension will be approximately proportional to changes in the average order parameter. Combining the data in Figures 5 and 9 with eq 7, furthermore, yields an estimate of ~200 dyn/cm for the area compressibility modulus that represents a reasonable value for PC bilayers in the fluid phase.[38]

4.4. Molecular Area. The preceding calculations support a mechanism by which the position of the double bond alters the lateral pressure profile within the bilayer, leading to a change in the molecular surface area. Such a mechanism predicts that the experimentally observed changes in ^{2}H NMR order parameter are due to changes in molecular dimension as opposed to local changes in the immediate vicinity of the double bond. The simulations support this view in that the order parameter profiles for the 16:0 *sn*-1 chain, replotted in Figure 10 with the mean order parameter for each isomer subtracted to better compare, have identical shape within statistical error. While it would seem that all four simulations, having been done with identical surface areas, would have the same average order parameter, this is not necessarily the case because the order parameter is actually probing the area per *sn*-1 chain. For the Δ^{15} isomer, as is evident from the order profile plotted in Figure 8a, the average order parameter of the *sn*-1 chain is slightly lower (implying larger area) than the other isomers, suggesting that the surface area requirement of the *sn*-2 chain is lower for Δ^{15} than the other systems. Thus, the analysis of the simulations supports the interpretation of the increase in experimental *sn*-1 order parameter, relative to the Δ^9 isomer, as resulting from a decreased surface area. Moreover, the simulations suggest that surface area requirements of the 18:1 *sn*-2 chain are largely independent of unsaturation position with the possible exception of the Δ^{15} system. Additional support for a decreased area for the *sn*-2 chain of the Δ^{15} isomer comes from Figure 9, where the data point for its lateral tension is somewhat higher than expected from eq 7.

The origin of the changes in molecular surface area can also be addressed by analyzing the results of the MD simulations. The NMR results for the positional isomers of [^{2}H$_{31}$]16:0-18:1PC showing increased order parameter and increased phase transition temperature upon moving the double bond toward either termini of the chain are similar to those seen when increasing acyl chain length in a series of saturated PC.[39] Therefore, one possibility is that the strength of acyl chain attractions is increased in the monounsaturated lipid as the double bond is shifted away from the center of the *sn*-2 chain, increasing the length of saturated chain segments above or below the double bond. To address this possibility, we examined the strength of the acyl chain interactions by computing the interchain (Lennard-Jones and electrostatic) contributions to the CHARMM force field from conformations saved during the simulation. The results presented in Figure 11 show that having the double bond in the middle of the chain is less energetically favorable than having a double bond nearer a terminus. It should be emphasized that the findings of these simulations, carried out under identical areas, likely underestimate the differences in acyl chain interactions. In the actual systems, the stronger attractions in the Δ^6 and Δ^{15} isomers would lead to reduced molecular area. The resulting increase in surface density would further increase the interaction energies beyond that observed in the simulation.

5. Summary

A combination of solid-state ^{2}H NMR and MD simulations was employed to investigate molecular organization in isomeric 16:0-18:1PC bilayers. The ^{2}H NMR spectra demonstrate that membrane order in the liquid crystalline state varies with the

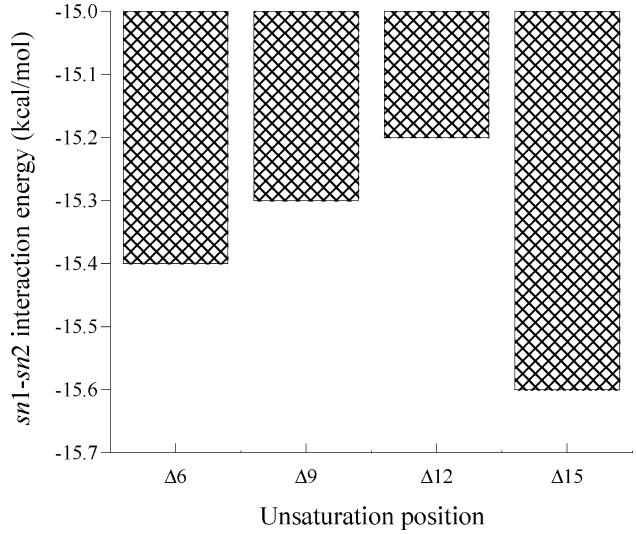

Figure 11. Interaction energy between the *sn*-1 and -2 acyl chains vs position of unsaturation for 16:0-18:1Δ^6PC, 16:0-18:1Δ^9PC, 16:0-18:1Δ^{12}PC, and 16:0-18:1Δ^{15}PC at 40 °C.

position of the double bond in a manner that parallels that seen for the temperature of the chain melting transition. As seen for the temperature of the gel to liquid crystalline transition T_m, the average order parameter $\bar{S}_{CD}$ for the [$^2H_{31}$]16:0 *sn*-1 chain in [$^2H_{31}$]16:0-18:1PC is lowest when the double bond is near the middle of the 18:1 *sn*-2 chain and increases when the double bond is shifted toward either end of the chain. The lateral tensions observed in the MD simulations are consistent with the area changes inferred from the experimental order parameters, assuming $K_A \sim 200$ dyn/cm. Thus, the simulations support the interpretation that the effect of position of the double bond is to change the molecular surface area. Analysis in terms of interaction energy, furthermore, is consistent with the hypothesis that a double bond located near the ends of the acyl chain allows more favorable chain−chain interactions between saturated segments.

Acknowledgment. It is a pleasure to thank Jenifer L. Thewalt for sharing her results with us, and to acknowledge the contribution to this research from Stephen P. Schuh and Sherrel D. Harris. The work was supported by a grant from the American Chemical Society Petroleum Research Fund (25340-B4) to S.R.W. and a grant from the National Science Foundation (MCB-0950258) to S.E.F.

References and Notes

(1) Lichesnstein, A. H. Dietary fat and cardiovascular disease risk: quantity or quality. *J. Women's Health* **2003**, *12*, 109–114.

(2) Stillwell, W.; Wassall, S. R. Docosahexaenoic acid: membrane properties of a unique fatty acid. *Chem. Phys. Lipids* **2003**, *126*, 1–27.

(3) Salem, N., Jr.; Litman, B.; Kim, H. Y.; Gawrsich, K. Mechanisms of action of docosahexaenoic acid in the nervous system. *Lipids* **2001**, *36*, 945–959.

(4) Coolbear, K. P.; Berde, C. B.; Keough, K. M. W. Gel to liquid-crystalline phase transitions of aqueous dispersions of polyunsaturated mixed-acid phosphatidylcholines. *Biochemistry* **1983**, *22*, 1466–1473.

(5) Niebylski, C. D.; Salem, N. A calorimetric investigation of a series of mixed-chain polyunsaturated phosphatidylcholines: effect of sn-2 chain length and degree of unsaturation. *Biophys. J.* **1994**, *67*, 2387–2393.

(6) Holte, L. L.; Peter, S. A.; Sinnwell, T. M.; Gawrisch, K. ^{2}H nuclear magnetic resonance order profiles suggest a change of molecular shape for phosphatidylcholines containing a polyunsaturated acyl chain. *Biophys. J.* **1995**, *68*, 2396–2403.

(7) Dratz, E. A.; Deese, A. J. The role of docosahexaenoic acid (22:6ω3) in biological membranes: examples from photoreceptors and model membrane bilayers. In *Health Effects of Polyunsaturated Fatty Acids in Seafoods*; Simopoulos, A. P., Kifer, R. R., Martin, R. E., Eds.; Academic Press: New York, 1986; pp 319−351.

(8) Smaby, J. M.; Momsen, M. M.; Brockman, H. L.; Brown, R. E. Phosphatidylcholine acyl unsaturation modulates the decrease in interfacial elasticity induced by cholesterol. *Biophys, J.* **1997**, *73*, 1492–1505.

(9) Holte, L. L.; Separovic, F.; Gawrisch, K. Nuclear magnetic resonance investigation of hydrocarbon chain packing in bilayers of polyunsaturated phospholpids. *Lipids* **1996**, *31*, S199–S203.

(10) McCabe, M. A.; Griffith, G. L.; Ehringer, W. D.; Stillwell, W.; Wassall, S. R. ^{2}H NMR studies of isomeric ω3 and ω6 polyunsaturated phospholipid membranes. *Biochemistry* **1994**, *33*, 7203–7210.

(11) Ehringer, W. D.; Belcher, D.; Wassall, S. R.; Stillwell, W. A comparison of α-linolenic acid (18:3ω3) and γ-linolenic acid (18:3ω6) in phosphatidylcholine bilayers. *Chem. Phys. Lipids* **1991**, *57*, 87–96.

(12) Stillwell, W.; Ehringer, W. D.; Dumaual, A. C.; Wassall, S. R. Cholesterol condensation of α-linolenic and γ-linolenic acid-containg phosphatidylcholine monolayers and bilayers. *Biochim. Biophys. Acta* **1994**, *1214*, 131–136.

(13) Barton, P. G.; Gunstone, F. D. Hydrocarbon chain packing and molecular motion in phospholipid bilayers formed from unsaturated lecithins. *J. Biol. Chem.* **1975**, *250*, 4470–4476.

(14) Huang, C.; Li, S. Calorimetric and molecular mechanics studies of the thermotropic phase behaviour of membrane phospholipids. *Biochim. Biophys. Acta* **1999**, *1422*, 273–307.

(15) Marsh, D. Thermodynamic analysis of chain-melting transition temperatures for monounsaturated phospholipid membranes: dependence on *cis*-monoenoic double bond position. *Biophys. J.* **1999**, *77*, 953–963.

(16) Scholfield, C. R.; Jones, E. P.; Nowakowska, J.; Selke, E.; Dutton, H. J. Hydrogenation of linolenate. II. Hydrazine reduction. *J. Am. Oil Chem. Soc.* **1961**, *38*, 208–211.

(17) Emken, E. A.; Scholfield, C. R.; Dutton, H. J. Chromatographic separation of *cis* and *trans* by argentation with a macroreticular exchange resin. *J. Am. Oil Chem. Soc.* **1964**, *41*, 388–390.

(18) Scholfield, C. R.; Emken, E. A. Isolation of methyl *cis*-15-octadecenoate by chromatography on a silver-treated macroreticular exchange resin. *Lipids* **1966**, *1*, 235–236.

(19) McCabe, M. A.; Wassall, S. R. Rapid deconvolution of NMR powder spectra by weighted fast Fourier transformation. *Solid State Nucl. Magn. Reson.* **1997**, *10*, 53–61.

(20) Davis, J. H.; Jeffrey, K. R.; Bloom, M.; Valic, M. I.; Higgs, T. P. Quadrupolar echo deuteron magnetic resonance spectroscopy in ordered hydrocarbon chains. *Chem. Phys. Lett.* **1976**, *42*, 390–394.

(21) Davis, J. H. The description of membrane lipid conformation, order and dynamics by ^{2}H NMR. *Biochim. Biophys. Acta* **1983**, *737*, 117–171.

(22) Seelig, J. Deuterium magnetic resonance theory and application to lipid membranes. *Q. Rev. Biophys.* **1977**, *10*, 353–418.

(23) Lafleur, M.; Fine, B.; Sternin, E.; Cullis, P. R.; Bloom, M. Smoothed orientational order profile of lipid bilayers by 2H-nuclear magnetic resonance. *Biophys. J.* **1989**, *56*, 1037–1041.

(24) Feller, S. E.; Gawrisch, K.; MacKerell, A. D., Jr. Polyunsaturated fatty acids in lipid bilayers: intrinsic and environmental contributions to their unique physical properties. *J. Am. Chem. Soc.* **2002**, *124*, 318–326.

(25) Feller, S. E.; Yin, D.; Pastor, R. W.; MacKerell, A. D., Jr. Molecular dynamics simulation of unsaturated lipid bilayers at low hydration: parameterization and comparison with diffraction studies. *Biophys. J.* **1997**, *73*, 2269–2279.

(26) Brooks, B. R.; Bruccoleri, R. E.; Olafson, B. D.; States, D. J.; Swaminathan, S.; Karplus, M. CHARMM: A program for macromolecular energy, minimization, and dynamics calculations. *J. Comput. Chem.* **1983**, *4*, 187–217.

(27) Klauda, J. B.; Brooks, B. R.; MacKerell, A. D.; Venable, R. M.; Pastor, R. W. An ab initio study on the torsional surface of alkanes and its effect on molecular simulations of alkanes and a DPPC bilayer. *J. Phys. Chem. B* **2005**, *109*, 5300–5311.

(28) Feller, S. E.; Brown, C. A.; Nizza, D. T.; Gawrisch, K. NOESY cross-relaxation rates and ethanol distribution across membranes. *Biophys. J.* **2002**, *82*, 1396–1404.

(29) Essmann, U.; Perera, L.; Berkowitz, M. L.; Darden, T.; Lee, H.; Pedersen, L. G. A smooth particle mesh Ewald method. *J. Chem. Phys.* **1995**, *103*, 8577–8593.

(30) Ryckaert, J. P.; G. Ciccotti, G.; Berendsen, H. J. C. Numerical integration of the cartesian equations of motion of a system with constraints: molecular dynamics of n-alkanes. *J. Comput. Phys.* **1977**, *23*, 327–341.

(31) Martinez-Seara, H.; Róg, T.; Pasenkiewicz-Gierula, M.; Vattulainen, I.; Karttunen, M.; Reigada, R. Effect of double bond position on lipid bilayer properties: insight through atomistic simulations. *J. Phys. Chem. B* **2007**, *111*, 11162–11168.

(32) Seelig, J.; Waespe-Sarcevic, N. Molecular order in cis and trans unsaturated phospholipid bilayers. *Biochemistry* **1978**, *17*, 3310–3315.

(33) Petersen, N. O.; Kroon, P. A.; Kainosho, M.; Chan, S. I. Thermal phase transitions in deuterated lecithins. *Chem. Phys. Lipids* **1975**, *14*, 343–349.

(34) Wang, Q.; Lin, H. N.; Li, S.; Huang, C. Calorimetric studies and molecular mechanics simulations of monounsaturated phosphatidylethanolamine bilayers. *J. Biol. Chem.* **1994**, *269*, 23491–23499.

(35) Wang, Q.; Lin, H. N.; Li, S.; Huang, C. Phosphatidylcholines with *sn*-1 saturated and *sn*-2 *cis*-monounsaturated acyl chains. Their melting behavior and structures. *J. Biol. Chem.* **1995**, *270*, 22738−22746.

(36) Soni, S. P.; Ward, J. A.; Sen, S. E.; Feller, S. E.; Wassall, S. R. Effect of trans unsaturation on molecular organization in a phospholipid membrane. *Biochemistry* **2009**, *48*, 11097–11107.

(37) Nagle, J. F. Area/Lipid of Bilayers from NMR. *Biophys. J.* **1993**, *64*, 1476–1481.

(38) Rawicz, W.; Olbrich, K. C.; McIntosh, T. J.; Needham, D.; Evans, E. A. Effect of chain length and unsaturation on elasticity of lipid bilayers. *Biophys. J.* **2000**, *79*, 328–339.

(39) Petrache, H. I.; Dodd, S. W.; Brown, M. F. Area per lipid and acyl length distributions in fluid phosphatidylcholines determined by ^{2}H NMR spectroscopy. *Biophys. J.* **2000**, *79*, 3172–3192.

JP105068G